Journal of Metals, Materials and Minerals, 36(4), e2568, 2026

Reducing water absorption of cement mortar by using modified clay brick waste

Nuntaporn KONGKAJUN[1,2], Somyote KONGKARAT[1,2], Wannasa PHUKUTNAM[1], Warittha SUJARITPANICH[1], Edward LAITILA[3], and Parinya CHAKARTNARODOM[4,*]

[1] *Department of Materials and Textile Technology, Faculty of Science and Technology, Thammasat University, Pathumthani, 12121, Thailand*
[2] *Thammasat University Research Unit in Sustainable Materials and Circular Economy, Thammasat University, Pathumthani, 12121, Thailand*
[3] *Department of Materials Science and Engineering, Michigan Technological University, Houghton, MI, 49931, USA*
[4] *Department of Materials Engineering, Faculty of Engineering, Kasetsart University, Bangkok, 10900, Thailand*

***Corresponding author e-mail**: fengpryc@ku.ac.th

Received date:
15 November 2025
Revised date:
1 April 2026
Accepted date:
2 July 2026

Keywords:
Clay brick waste;
Hydrophobic;
Stearic acid;
Mortar

Abstract

Cement mortar is inherently hydrophilic due to its porous structure, which allows water penetration and adversely affects its durability and long-term performance. To mitigate this issue, hydrophobic cementitious materials can be developed by incorporating hydrophobic substances during mixing to provide hydrophobic properties throughout the material, achieved by introducing a wet chemical method using stearic acid-modified clay brick waste (MCBW) as a hydrophobic agent. The MCBW is prepared by treating clay brick waste with stearic acid (SA) and subsequently used as a partial replacement for fine aggregates. The effects of the MCBW incorporation on compressive strength and water resistance are investigated. When 30% of fine aggregate is replaced by MCBW (by weight), the optimized mortar showed substantial improvements: its 28 day cured compressive strength increased by 12% compared to the control, while achieving water resistance. Hydrophobic behavior is confirmed by a water contact angle of 145° and a significant reduction in the water penetration rate. Microstructural and thermal analyses (SEM and TG/DTG) further revealed that the incorporation of MCBW promotes cement hydration, contributing to improved performance.

1. Introduction

Cement is inherently hydrophilic due to its porous structure, making it susceptible to deterioration when exposed to environmental conditions overtime. The ingress of water, along with the corrosive effects of chlorides or sulfates, significantly compromises its durability and long-term performance. These processes can initiate corrosion of reinforcement steel, sulfate attack, and freeze-thaw damage, increasing maintenance and repair costs [1–3]. To mitigate these issues, hydrophobic cement has been developed to repel water, thereby enhancing durability and reducing maintenance requirements [4]. Consequently, hydrophobic cement and concrete are widely employed in moisture-sensitive applications, including underground structures, roofing systems, bridges, and marine or cold-region environments [5,6].

To effectively reduce the hydrophilic nature of concrete, hydrophobic cementitious materials can be implemented through two primary approaches: surface treatment and integral modification. Surface treatment involves creating a thin hydrophobic layer using agents such as silane-based solutions or nano-modified organic-inorganic composites, which significantly reduce water absorption [7,8]. In contrast, integral modification incorporates hydrophobic substances directly into the mix during concrete production. This method provides water-repellent properties throughout the bulk material. This approach offers a key advantage over surface coatings by preventing the risk of coating degradation and ensuring more durable, long-term protection. Beyond simple water repellency, hydrophobic mortar exhibits enhanced resistance to chloride ion penetration and sulfate attack. By limiting concrete water ingress, chloride transport to reinforcement steel is reduced, thereby preventing corrosion, expansive rust formation, and surface spalling. Additionally, improved water resistance restricts the penetration of sulfate-rich fluids, slowing their reactions with calcium hydroxide and the subsequent formation of expansive ettringite, which can induce internal cracking. [9,10].

The construction industry generates substantial quantities of construction and demolition waste (CDW) including clay bricks and tiles, each year. The effective utilization of CDW is a key strategy for reducing the demand for natural resources such as river and marine sand [11–13]. The extraction of natural sand has significant environmental impacts, including accelerating erosion, diminishing protection against storm surges and contributing to saltwater intrusion. Previous studies have investigated the use of crushed clay bricks waste as an aggregate. Clay brick waste (CBW) can partially replace natural fine aggregates in mortar mixes [14,15], and its fine powder fraction can act as a filler to reduce the pore structure. However, CBW poses certain challenges: it is more porous and exhibits higher water absorption than natural aggregates. Consequently, a higher water-cement ratio in the mix is needed, which can affect workability and overall mix performance. Moreover, high replacement levels of sand with CBW have been associated with reductions in the compressive strength of mortar [14,16,17].

To mitigate the water absorption of cement-based materials, researchers have recently focused on developing hydrophobic

modifications of various waste powders, enabling their use as a hydrophobic agent [18]. Previous studies have investigated stearate compounds such as calcium stearate and aluminum stearate as waterproof agents [19–21]. The results demonstrated that at low stearate compound concentrations can improve the compressive strength and enhance water repellency of the resulting cement paste relative to the OPC sample. Furthermore, the presence of calcium stearate was shown to enhance the hydration reaction of cement.

Recently, many researchers have focused on using stearic acid for hydrophobic modification of various alternative materials, including oyster shells, metakaolin, mica, for potential use in concrete aggregates [6,22,23]. A key advantage of employing stearic acid is its cost-effectiveness. For instance, Song *et al.* reported that incorporating modified oyster shells into mortar resulted in a 29% decrease in water absorption compared with ordinary mortar [6]. Furthermore, the addition of this modified oyster shell enhanced the corrosion resistance of mortar.

Many studies have demonstrated the effectiveness of using stearic acid to hydrophobically modify alternative cementitious materials. Yang *et al*. investigated the effect of stearic acid-modified metakaolin on the properties of cement mortar [22]. They reported a 36.24% reduction in water absorption and a 14.23% increase in compressive strength under dry-wet cycling sulfate attack for modified mortar. Pang *et al.* reported that using a stearic acid content of 3% to 5% resulted in modified mica having a water contact angle greater than 120°, which corresponded to a 64% decrease in the water absorption of the modified mortar [23].

The present study proposes the use of stearic acid-modified CBW to produce a hydrophobic mortar through integral modification. The porous structure of CBW provides an anchorage site for stearic acid, improving its loading efficiency, and enhancing the hydrophobic performance compared with conventional mixing approaches. In addition, by regulating water resistance, the modification ensures the cement paste remains hydrated over a longer period, supporting continued hydration while promoting the development of the calcium silicate hydrate (C–S–H) gel structure. The utilization of CBW in mortar offers a dual purpose: it offers an effective way to manage a large amount of construction and demolition waste while simultaneously decreasing the demand of virgin raw materials. Thus, presenting an environmentally friendly method to recycle waste and provide an effective technique for improving mortar durability.

2. Experimental

2.1 Materials

In this study, Portland limestone cement (PLC), sand, and clay brick waste (CBW) were used. Table 1 represents the chemical compositions of each raw materials by X-ray fluorescence (XRF: Bruker S2 PUMA Series II) test. Portland limestone cement (PLC), a blended hydraulic cement defined by ASTM C595 [24] is used in this study to reduce CO_2 emissions by approximately 10%. River sand and CBW passing a 2.36 mm sieve were used as fine aggregate. The particle size distribution curve of fine aggregates is provided in Figure 1. Stearic acid (SA) and ethanol were bought from Qrec chemical company, New Zealand. Particle size distribution of fine aggregates are analyzed by ASTM C136 sieve analysis [25]. The CBW was supplied by a clay brick factory in Thailand. The specific gravity of river sand, and CBW are given in Table 2. Specific gravity measurements of fine aggregates was carried out in accordance with ASTM D854 by water pycnometer [26].

2.2 Synthesis of modified clay brick waste

Stearic acid is used as a modifier. To determine the effect of SA on the modified CBW, varying amounts of SA (from 0% to 5% by mass of CBW) was stirred in the 100 mL ethanol solution with a magnetic stirrer for about 15 min to obtain a mixed solution at temperature at 50°C. Then, the SA solution was cooled to room temperature. The CBW was soaked in the solution for 30 min and stirred to obtain modified CBW (MCBW). The MCBW was dried at 60°C for 24 h.

2.3 Preparation of hydrophobic mortar

The mix proportions of the hydrophobic mortar are listed in Table 3. The MCBW with the optimal dosage of SA is used to replace river sand in the mortar (water-to-cement (W/C) ratio = 0.5) at replacement levels of 0%, 10%, 20%, 30% and 40% by mass of sand. The raw materials were weighed and mixed thoroughly by Hobart mixer. After mixing, the mortar was cast into a 50 mm × 50 mm × 50 mm cube mold. Then, the specimens were air cured for 7 day and 28 day.

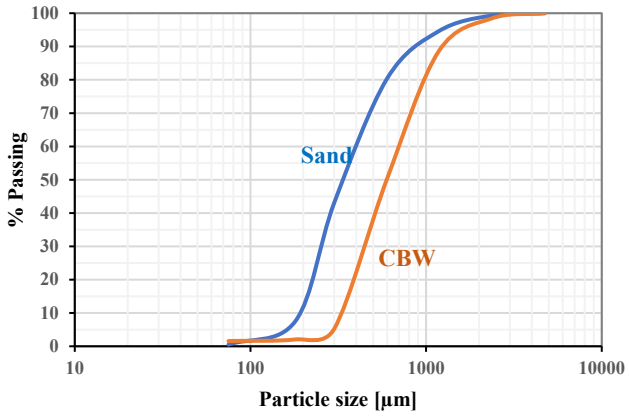

Figure 1. Particle size distribution of raw materials.

Table 1. Chemical composition of raw materials.

Main oxide [%]	CaO	SiO_2	Al_2O_3	Fe_2O_3	SO_3	MgO	Na_2O	K_2O	TiO_2
PLC	70.98	16.77	3.22	3.28	4.21	0.78	0	0	0
CBW	0.6	22.87	68.32	5.24	0	0.1	0.1	1.85	0
Sand	0.15	96.29	2.12	1.01	0	0	0	0.25	0.18

Table 2. Specific gravity of sand and CBW.

Fine aggregates	Specific gravity
Sand	2.652
CBW	1.985

2.4 Testing procedure

2.4.1 Characterization of MCBW

The hydrophobicity of the MCBW is determined by a contact angle meter (Theta lite Optical tensiometer, TL100). A compacted MCBW sample was prepared by pressing at 50 MPa to form a 12 mm diameter disc. A 5µL water droplet was deposited onto a compacted MCBW sample. Fourier transformation infrared spectroscopy (FT-IR, Shimadzu) was used to determine the functional groups adsorbed on the surface of MCBW. The phase analysis of CBW and MCBW are determined using X-ray diffraction (XRD, PANalytical Empyrean, X-ray diffractometer). The XRD data was collected between 10° and 70° 2θ.

2.4.2 Characterization of the modified mortars

The compressive strength of the mortar is evaluated in accordance with ASTM C109 [27] at curing ages of 7 day and 28 day. Bulk density and water absorption are determined following ASTM C642 [26] . Cubic specimen with dimensions of 50 mm × 50 mm × 50 mm were prepared, with five specimens for each mixture. Water penetration is determined by Karsten tube method, in which the tube was sealed to the specimen surface to monitor water penetration over time; readings were recorded at 15 min intervals. The water contact angle (WCA) of MCBW and different types of mortar samples is determined using a contact angle meter. Prior to testing, the mortar samples were dried at 60°C for 24 h and their surfaces were cleaned. Five samples were measured for each MCBW content. The reported values represent the average.

For microstructural characterization, phase and thermal analysis, the broken pieces from post-mechanical testing were collected. These samples were soaked in ethanol for 24 h to stop the hydration reaction and oven dried. The microstructure of mortar samples after curing 28 day are observed with scanning electron microscope (SEM, JEOL JSM-64OLV). In phase and thermogravimetric analysis, the samples were crushed and ground to powders passing through a 100 mesh sieve. Thermogravimetric analysis (TG/DTG, Netzsch STA509 Jupitor) is used to analyze the effect of MCBW content on hydration of cement. The 28 day cured mortars were heated in a nitrogen gas atmosphere from 30°C to 1000°C at a heating rate of 10°C·min^{-1}.

3. Results and Discussion

3.1 Effects of stearic acid content on the water contact angle

The water contact angle (WCA) of the MCBW changes with the concentration of SA, Figure 2. At a low SA content (0% to 2%), the MCBW samples showed a consistent low WCA of 20° to 50°, indicating a hydrophilic (water-attracting) surface. A sharp increase in the WCA is observed as the SA content rose from 2% to 3%, with the angle increasing to approximately 150°. For the SA concentrations above 3%, the WCA is stable, demonstrating a clear transition to a hydrophobic (water-repelling) surface. This data suggests that 3% is the optimal SA concentration for achieving stable hydrophobic properties in MCBW. The wettability of CBW before and after modification is observed in Figure 3. Generally, water absorption of the commercial clay brick is between 10% and 20% due to its internal porosity [14,28]. Thus, the wettability of CBW before modification, as shown in Figure 3(a), presented hydrophilic properties with a low WCA of 19.6 ± 3.7°. After modification by stearic acid, the wettability of MCBW, Figure 3(b), indicated hydrophobic properties with a high WCA of 153.3 ± 0.2°.

The changes in functional groups before modification (a), after modification (b), and for stearic acid (c), are characterized using FT-IR data, Figure 4. Compared with before modification of CBW, the FT-IR spectra of MCBW presented a band at approximately 2916 cm^{-1} and 2847 cm^{-1}, which is related to the stretching vibration of –CH_2 and –CH_3. The major functional group consisting of the carboxyl group which is related to C=O stretching vibration of –COOH at 1699 cm^{-1} is also observed in the MCBW. Thus, it can be concluded that these functional groups of SA are placed onto the CBW surface, and these results correspond to hydrophobic properties of MCBW seen in Figure 3(b).

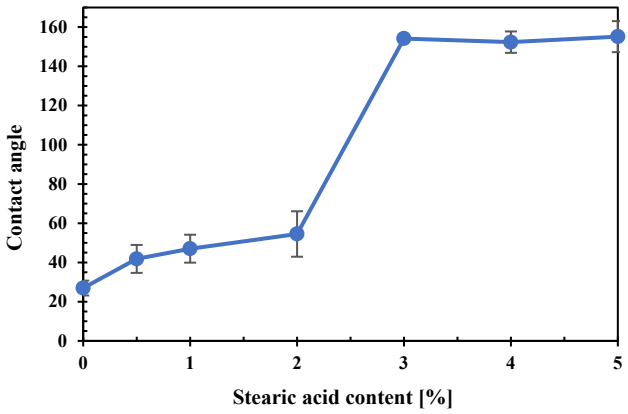

Figure 2. The water contact angle of CBW with the SA contents.

Table 3. Mix proportions of mortar.

Mix	PLC [g]	Water [g]	Sand [g]	MCBW [g]	Plasticizer [g]
Control	300	150	480	0	1.5
10MCBW	300	150	432	48	1.5
20MCBW	300	150	384	96	1.5
30MCBW	300	150	336	144	1.5
40MCBW	300	150	288	190	1.5

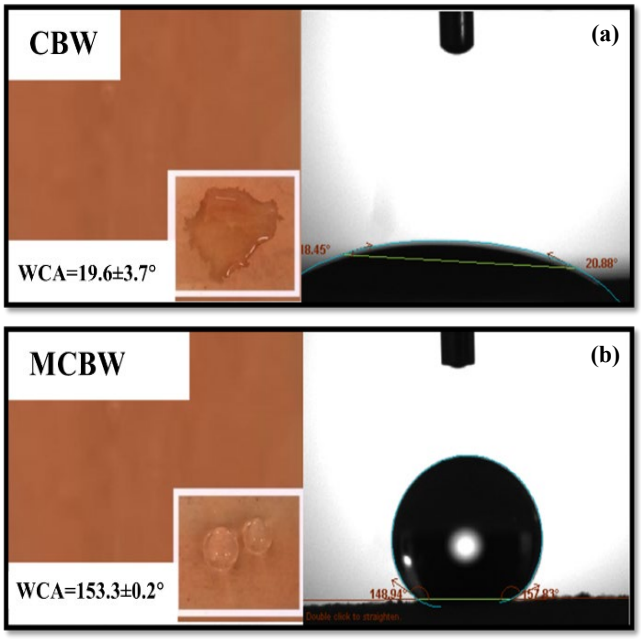

Figure 3. The images for the wettability of (a) CBW, and (b) MCBW.

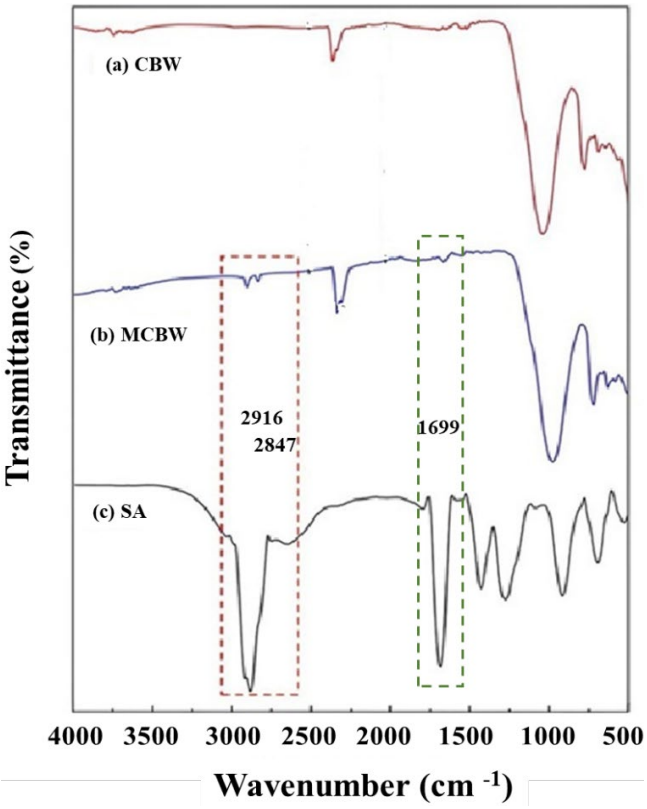

Figure 4. FT-IR spectra of (a) CBW, (b) MCBW, and (c) stearic acid (SA).

3.2 Characterization of modified mortar

The XRD patterns, Figure 5, of the CBW and MCBW show the main component of CBW is quartz, muscovite, sanidine and Fe_2O_3, and no new diffraction peaks are observed in the pattern of MCBW. This indicated that the crystalline phase in CBW is not changed after the modification by 3% stearic acid.

3.2.1 Mechanical and physical properties

The compressive strength for the cement mortars is illustrated in Figure 6, with all mixes exhibited an expected increase in compressive strength with curing time. The control mix reached compressive strengths of 35 MPa and 39 MPa at 7 day and 28 day, respectively. Compared with the control, the strengths of 10MCBW, 20MCBW, and 30MCBW mixes increased by 5.4%, 6.7%, and 12%, respectively. An overall enhancement in compressive strength is observed with increasing MCBW content up to 30% replacing sand, with the 30MCBW mix at 28 day showing the highest strength (12% improvement). This improvement can be attributed to the pozzolanic activity of CBW, which promotes the secondary formation of C–S–H gel over time, resulting in a denser microstructure and improving long-term strength development [17]. In addition, the presence of stearic acid on the MCBW surface reduces water absorption by the aggregates, allowing more water to remain available within the cement matrix for the long-term hydration of the cement particles, thereby contributing to higher compressive strength [21]. However, as the MCBW content increased from 30% to 40%, a reduction in compressive strength is observed. The reduction in compressive strength of 40MCBW mix is attributed to the intrinsic characteristics of recycled aggregates from construction waste such CBW, which may contain surface cracks and defects [29].

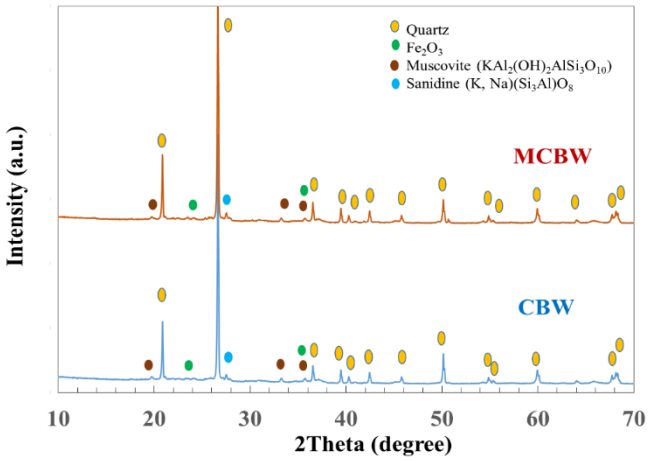

Figure 5. XRD patterns of the clay brick waste before modification (CBW) and after modification with 3% SA content (MCBW).

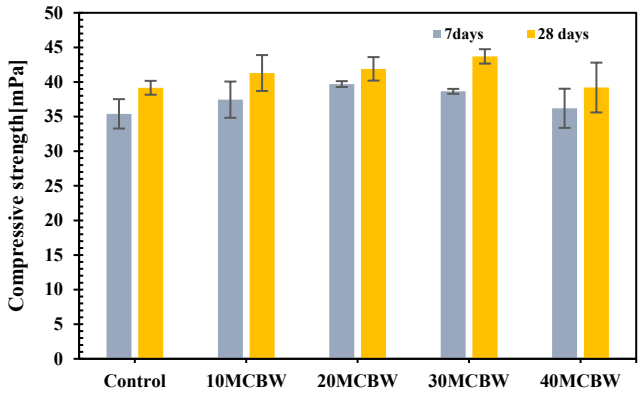

Figure 6. Compressive strength development of cement mortar incorporating varying levels of MCBW cured at 7 day and 28 day.

Furthermore, the larger particle size, Figure 1, and porous nature of the CBW compared with sand can introduce additional voids into the mortar structure. Therefore, the optimal MCBW replacement level for sand is suggested to be 30%.

The effect of MCBW content on the bulk density of the cement mortar is illustrated in Figure 7. As expected, a slight decrease in bulk density was about 1.51%, in comparison to the control formula when the MCBW content is increased. The reason is the porous nature and lower specific gravity, Table 2, of clay brick comparing with sand which can affect the bulk density of cement mortar [28].

3.2 Water resistance

The effect of MCBW content on the water absorption of the mortar is presented in Figure 8. A significant reduction in water absorption is observed with increasing MCBW content. Compared with the control mix, water absorption decreased by 40.4%, 61.7% and 75.6% for the 10MCBW, 20MCBW, and 30MCBW mixtures, respectively, indicating the effective development of water-repellent properties with the incorporation of MCBW. This improvement is attributed to the formation of a water repellent layer that limits water penetration. Two key mechanisms govern this behavior. Capillary blocking occurs as hydrophobic coating disrupts the continuity of pore networks, thereby restricting water transport and reducing sorptivity. In addition, the reduction in surface energy increases the contact angle between water and pore surfaces, which diminishes capillary suction. However, increasing the MCBW content from 30% to 40% did not result in further improvement in water resistance. This is due to the increased porosity of the mortar mix at higher replacement levels. The crushing and milling processes used to produce recycled aggregates can introduce microcracks with in the aggregates [30]. Consistent with previous studies, excessive microcracking and porosity can facilitate water penetration, leading to increased water absorption in mortar [18].

The relationship between water penetration and time of mortar samples cured for 28 das, is illustrated Figure 9(a) as measured by the Karsten tube test, while Figure 9(b) shows calculated water penetration rates for different MCBW contents. The experimental setup on the mortar surfaces is shown in Figure 9(c). The results indicate that water penetration is proportional to the square root of time, consistent with previous studies [31,32]. Accordingly, the water penetration rate is determined from the slope of the fitted line over the test duration (t = 0 to 180 min, corresponding to t1/2 = 0 to 109.3 $sec^{1/2}$).

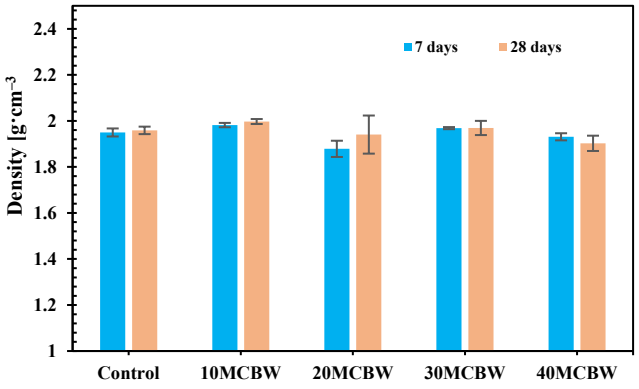

Figure 7. Bulk density of cement mortar incorporating varying levels of MCBW cured at 7 day and 28 day.

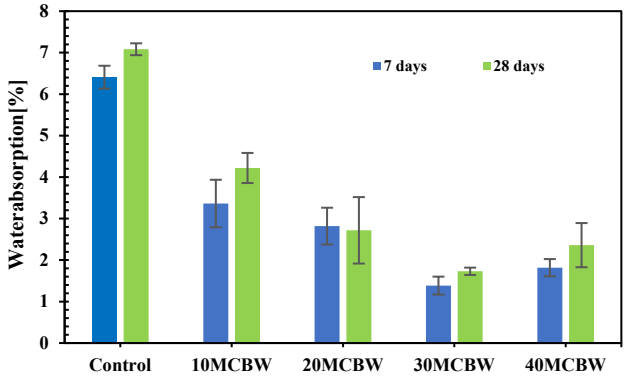

Figure 8. Water absorption of cement mortar incorporating varying levels of MCBW cured at 7 and 28 day.

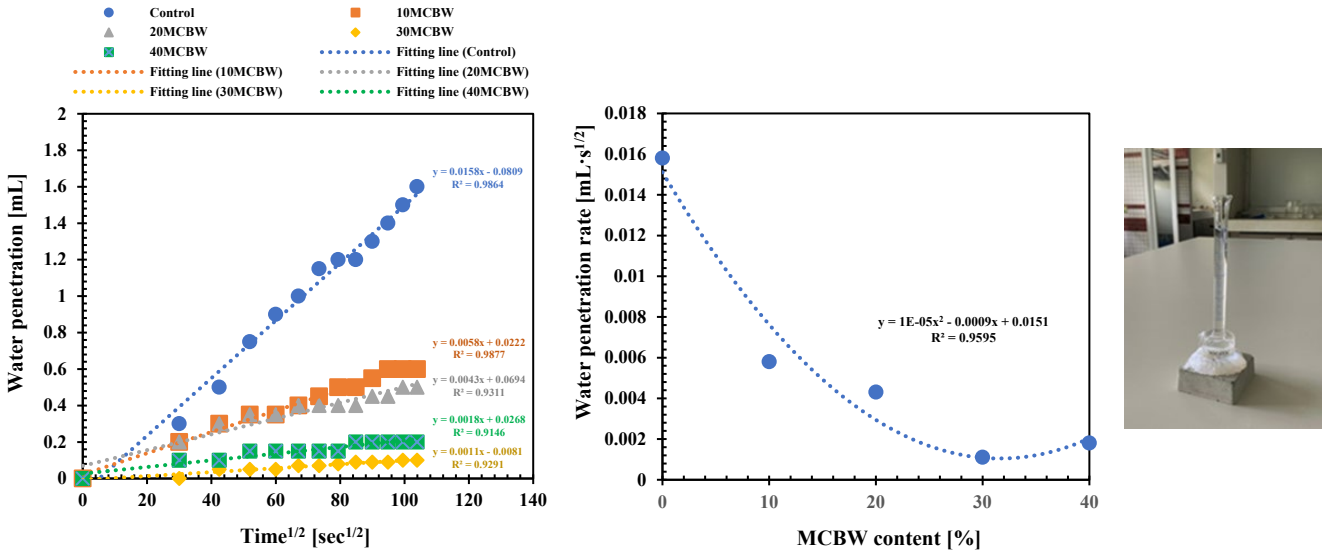

Figure 9. (a) A relationship between water penetration and time of mortar samples cured at 28 day, and (b) calculated water penetration rates for different MCBW contents, and (c) Karsten tube test.

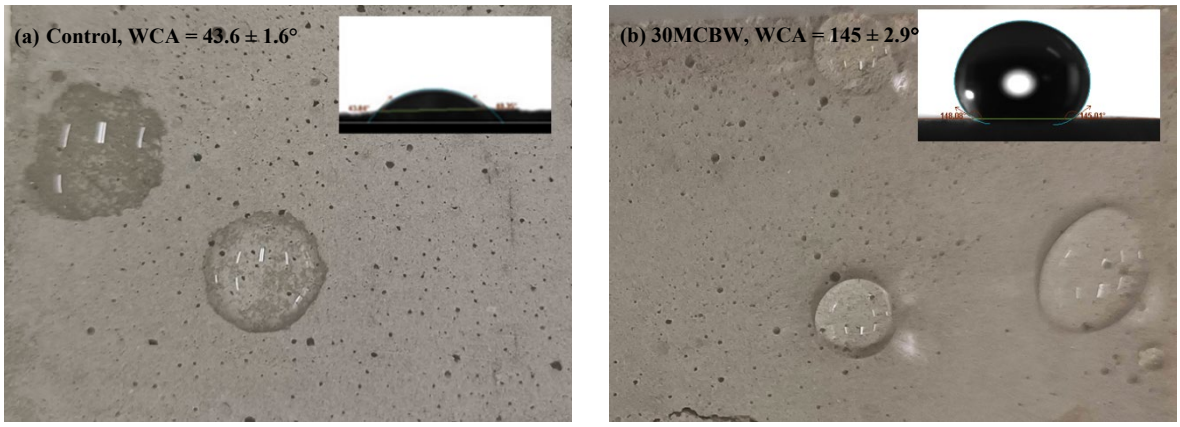

Figure 10. The water contact angle of the mortars (a) control formula, and (b) 30MCBW.

The control mortar exhibited a relatively high-water penetration rate of 0.0158 mL·min^{-1}, as shown in Figure 9(a). In contrast, mortars containing 10%, 20%, 30%, and 40% MCBW showed significantly lower rates of 0.0058 mL·min^{-1}, 0.0043 mL·min^{-1}, 0.0011 mL·min^{-1}, and 0.0018 mL·min^{-1}, respectively. These correspond to reductions of 63.3%, 72.8%, 93.0%, and 88.6% compared with the control. The improved water resistance of MCBW-modified mortars is attributed to the formation of a hydrophobic lining within the pore structure, which acts as a barrier to capillary suction [30]. The mortar containing 30% MCBW exhibited the greatest reduction in water penetration (93%). However, increasing the MCBW content to 40% did not yield further improvement, consistent with the trends observed for water absorption. The water penetration rate generally decreases with increasing MCBW content up to an optimal level of 30%, Figure 9(b). As discussed in Section 3.2, capillary water uptake is strongly influenced by the internal pore structure and microcracks within the aggregates [29,30]. At higher replacement levels, increased porosity within the mortar matrix likely counteracts the hydrophobic effect, leading to a slight increase in water penetration.

The water contact angle of the mortar without and with MCBW can be observed in Figure 10. The water contact angle of 43.6 ± 1.5° at MCBW content of 0%, while values of 145 ± 2.9° is determined at 30% MCBW. The water contact angle of the unmodified mortar exhibits hydrophilic properties as seen in Figure10 (a). When 30% of the MCBW is incorporated (Figure 10(b)), the water contact angle significantly increased showing the change from hydrophilic to a hydrophobic state. This confirms that the MCBW can form a hydrophobic lining on the pore walls of mortar to prevent water penetration, increasing the water contact angle.

3.3 Chemical composition and microstructural characterization

Analysis of the XRD patterns can characterize the phase composition of the mortars after 28 day of curing. The XRD patterns of the mortar samples with varying MCBW contents are plotted in Figure 11 with phases identified. All mortar samples contain similar hydration products, including ettringite, calcium hydroxide (Portlandite, $Ca(OH)_2$), calcium silicate hydrate (C–S–H) and $CaCO_3$. This indicates that the addition of MCBW into the mortar did not alter the type of hydration products formed within the cementitious matrix.

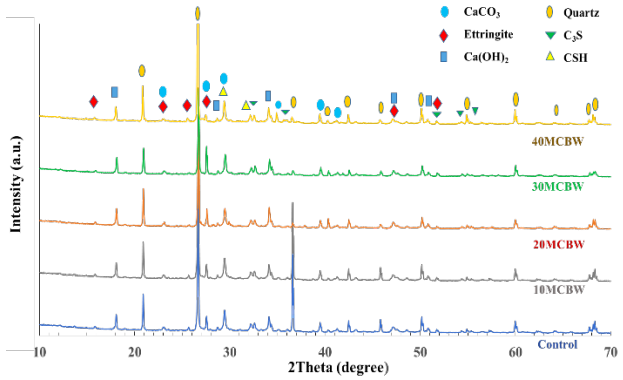

Figure 11. XRD patterns of the mortar samples with 0%, 10%, 20%, 30% and 40% MCBW content.

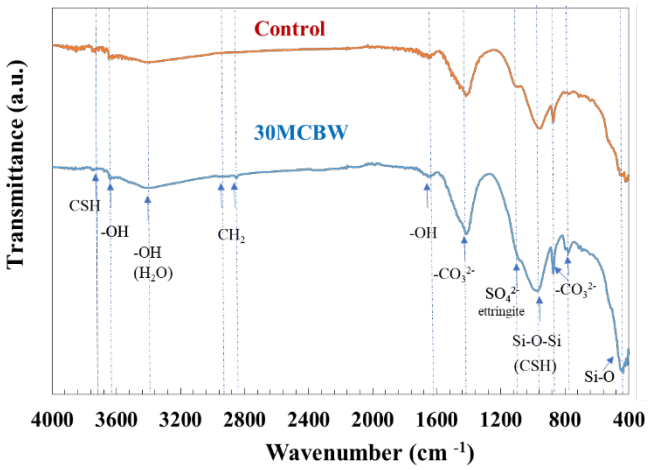

Figure 12. FT-IR spectra of control formula and 30MCBW sample.

The FT-IR spectrum can be used to characterize the hydration products and the presence of the modifying agent in the 28 day hydrated mortars, Figure 12. The spectra confirmed the presence of hydration products: C–S–H, calcium hydroxide, calcium carbonate and ettringite. The strong peaks of calcium hydroxide –OH stretching vibration are also visible at 3635 cm^{-1}. The broad band in the 3500 cm^{-1} to 3000 cm^{-1} region of the spectra is attributed to the symmetric and asymmetric stretching of the O–H vibration of the water molecules within C–S–H gels [33]. The characteristic Si–O–Si stretching mode at 945 cm^{-1} confirmed the formation of C–S–H phase. The presence of

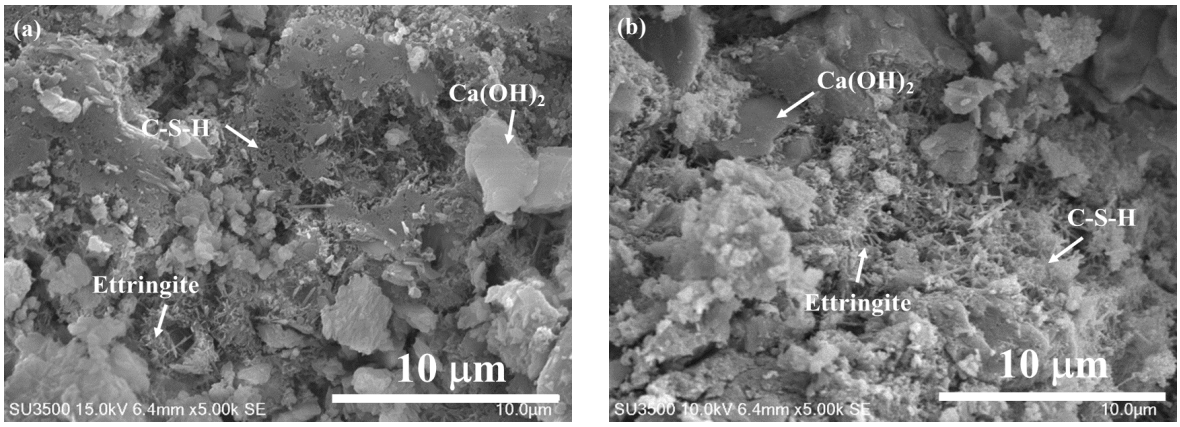

Figure 13. SEM images of (a) control formula and (b) 30MCBW sample.

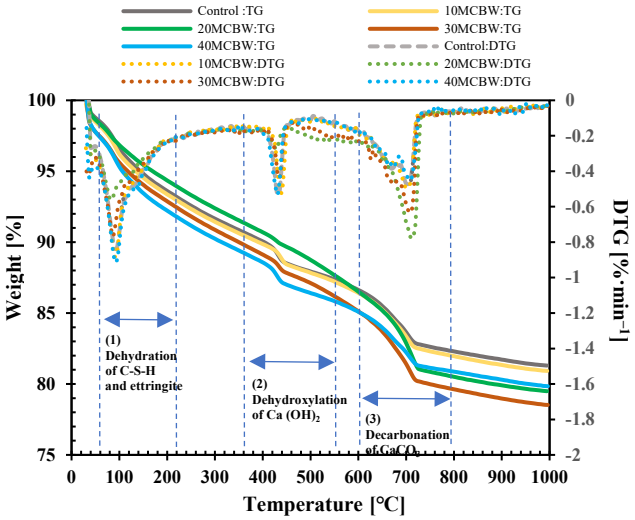

Figure 14. TG/DTG analysis of the mortar samples with 0 %, 10 %, 20 %, 30 % and 40 % MCBW content.

asymmetric stretching vibration and bending vibration of the carbonate $–CO_3^{2–}$ is detected at 1425 $cm^{–1}$ and 875 $cm^{–1}$. Moreover, the existence of ettringite is indicated by the $–SO_4^{2–}$ stretching vibration detected around 1100 $cm^{–1}$. In mortar samples 30MCBW, a distinct peak related to the organic modifier is detected. The $–CH_2$ and $–CH_3$ stretching vibration are observed at 2916 $cm^{–1}$ and 2847 $cm^{–1}$ and the carboxyl (COO–) stretching vibration is identified at 1675 $cm^{–1}$. The results indicate that the mortar is modified by stearic acid.

The SEM images illustrate the microstructural differences between the control mortar and the modified mortar with 30% MCBW, Figure 13. The surface of the unmodified control mortar (Figure 13(a)) primarily showed typical hydration products including $Ca(OH)_2$, C–S–H gel, and needle-like ettringite. The overall structure appeared loose and contained large pores. In contrast, the microstructure of the mortar containing 30% MCBW (Figure 13(b)) revealed a greater amount of hydration products, specifically more C–S–H gel, $Ca(OH)_2$ and denser formations of needle-like ettringite. This high concentration of hydration phases contributes to enhanced structure compaction and reduced the porosity. This denser packing of the hydrated cement paste is beneficial, leading to the higher compressive strength observed in the modified mortar compared to the control sample.

3.4 Thermal analysis

To further investigate the effect of the MCBW on the hydration reaction of mortars, thermogravimetric analysis (TG) and its derivative (DTG) are used to quantify the presence of hydration products in the mortar samples. The TG/DTG results, Figure 14, of the mortars with various MCBW contents reveals three main stages of weight losses as the mortar samples are exposed to elevated temperatures, corresponding to the dehydration, dehydroxylation, and decarbonation of various hydration products such as C–S–H, ettringite, and $Ca(OH)_2$ [34–36]. The DTG peaks indicate the rate of weight loss for each stage.

Stage 1 is the initial weight loss (Ldh) (30°C to 200°C), associated with the dehydration of bound water from the C–S–H and ettringite. Stage 2 is the weight loss (350°C to 550°C), which corresponds to the dehydroxylation of Portlandite ($Ca(OH)_2$) (Ldx). Weight loss of stage 1 and stage 2 could reflect the C–S–H, ettringite, and $Ca(OH)_2$ content produced by hydration reaction of cement. Stage 3 is the final weight loss (600°C to 800°C), which is due to the decarbonation of calcium carbonate ($CaCO_3$) (Ldc). Since, $CaCO_3$ primarily forms by carbonation of $Ca(OH)_2$. Thus, the Ldc value can indirectly reflect the amount of $Ca(OH)_2$ produced by hydration reaction [34].

Table 4. The weight losses of mortars with various MCBW contents in different temperature ranges.

Samples	Weight loss [%]			Chemically bound water	Degree of hydration,
	L_{dh}	L_{dx}	L_{dc}	(W_B)	∝ (%)
	30°C to 200°C	350°C to 550°C	600°C to 800°C		
Control	6.39	3.48	4.33	11.64	48.52
10MCBW	6.63	3.42	4.45	11.87	49.47
20MCBW	5.65	3.88	6	11.99	49.95
30MCBW	7.14	3.84	5.47	13.22	55.09
40MCBW	7.81	3.57	4.2	13.10	54.59

Based on the TG/DTG curves, the weight losses corresponding to the hydrated compounds, dehydration (Ldh), dehydroxylation (Ldx) and decarbonation (Ldc), are defined by the three temperature ranges presented in Table 4. The amount of chemically bound water (WB) is calculated using the weight losses from three stages, as shown in Equation (1). In this equation, the value of 0.41 is a conversion factor to estimate the WB and derived from carbonated Portlandite [35]. The calculated degree of hydration ($\propto$) is subsequently determined according to Equation (1) and Equation (2). The value of 0.24 in Equation (2) represents the maximum amount of chemically bound water required to fully hydrate a cement 1 g [35,36].

$$WB = Ldh + Ldx + 0.41\ Ldc. \quad (1)$$

$$\propto = (WB / 0.24) \quad (2)$$

A summary, Table 4, of the weight losses of mortars with varying MCBW contents across the temperature range are provided. Compared with the control, the weight loss in stage 1(Ldh) and stage 2 (Ldx), which correspond to the dehydration of bound water from C–S–H/ ettringite and dehydroxylation of $Ca(OH)_2$, increased as the MCBW content is raised. This trend indicates that the modified mortars generated a higher content of hydration products (C–S–H, ettringite and $Ca(OH)_2$) compared to the control sample. In stage 3 (Ldc) 600°C to 800°C, the weight loss due to $CaCO_3$ decarbonation initially increased with MCBW content up to 20%. However, upon further increasing the MCBW content beyond 20%, the weight loss associated with $CaCO_3$ began to decrease. This inhibitory effect on carbonation aligns with previous studies where an excessive amount of SA in the MCBW inhibited the carbonation of calcium hydroxide [18].

The calculated degree of hydration for the modified mortars increased from 48.52% for the control mix to 55.09% with the incorporation of 30% MCBW using Equation (1) and Equation (2). This enhancement indicates that the presence of 30% MCBW promotes cement hydration, facilitating the formation of C–S–H, ettringite and $Ca(OH)_2$. The stearic acid coating on the MCBW surface plays a key role by reducing water absorption by the fine aggregates and effectively conserving water within the cement matrix, thereby supporting the overall continued hydration reaction [21] . Consistent with this behavior, the mortar containing 30% MCBW also achieved a 12% increase in compressive strength compared with the control. However, further increasing the MCBW content to 40% resulted in a slight reduction in the calculated degree of hydration to 54.59%. This trend aligns with previous studies, which suggest that excessive stearic acid could begin to hinder cement hydration by interfering with the reaction processes within the cement matrix [6,18,37].

4. Conclusions

It has been established that stearic acid–modified clay brick waste (MCBW) can successfully be utilized as a partial replacement for nature fine aggregates to produce hydrophobic mortar through an integral modification approach. The results demonstrate that incorporating MCBW significantly enhances water resistance and improves mechanical performance.

The incorporation of MCBW reduced water absorption and water penetration, primarily owing to the formation of a hydrophobic lining within the pore structure. This behavior is governed by capillary blocking and surface energy reduction, which together limit water ingress and suppress capillary suction. Among the investigated mixtures, the mortar containing 30% MCBW exhibited the most pronounced improvement, achieving reductions of up to 75.6% in water absorption and demonstrating strong hydrophobic behavior, with a water contact angle reaching 145° compared with the control. In terms of mechanical properties, compressive strength increased with the MCBW content up to 30%, reaching a maximum improvement of 12%. This enhancement is attributed to improved internal moisture retention, which supports continued cement hydration. The calculated degree of hydration, derived from TG/DTG analysis, further confirmed this trend, with the highest value observed at 30% MCBW. Microstructural observations using SEM corroborated these findings, revealing increased formation of C–S–H gel and needle-like ettringite in the modified mortar.

Overall, the proposed approach not only enhances mortar durability but also provides a sustainable solution for recycling construction and demolition waste, thereby reducing dependence on natural sand and supporting environmentally responsible construction practices.

Acknowledgements

This work was supported by Thammasat University Research Unit in Sustainable Materials and Circular Economy.

References

[1] H. Higashiyama, K. Yamauchi, M. Sappakittipakorn, M. Sano, and O. Takahashi, "A visual investigation on chloride ingress into ceramic waste aggregate mortars having different water to cement ratios," *Construction and Building Materials,* vol. 40, pp. 1021–1028, 2013.

[2] K. Ram, M. Serdar, D. Londono-Zuluaga, and K. Scrivener, "The effect of pore microstructure on strength and chloride ingress in blended cement based on low kaolin clay," *Case Studies in Construction Materials,* vol. 17, p. e01242, 2022.

[3] N. Sharma, and P. Sharma, "Effect of hydrophobic agent in cement and concrete : A Review," *IOP Conference Series: Materials Science and Engineering,* vol. 1116, no. 1, p. 012175, 2021.

[4] Z. Dai, H. Guo, Y. Wang, M. Wang, Y. Zhang, and K. Qian, "Mechanically strength with water repellency: Recently advances in superhydrophobic concrete," *Journal of Cleaner Production,* vol. 491, p. 144839, 2025.

[5] S. Mu, T. Wang, G. Liu, M. Jin, L. Liu, H. Tan, and Q. Ma, "Durability evaluation and microstructure optimization of spray concrete for undersea tunnel: Role of hydrophobic agent and densifying material," *Construction and Building Materials,* vol. 489, p. 140591, 2025.

[6] Q. Song, Q. Wang, S. Xu, J. Mao, X. Li, and Y. Zhao, "Properties of water-repellent concrete mortar containing superhydrophobic oyster shell powder," *Construction and Building Materials,* vol. 337, p. 127423, 2022.

[7] J. González-Coneo, R. Zarzuela, F. Elhaddad, L. M. Carrascosa, M. L. A. Gil, and M. J. Mosquera, "Alkylsiloxane/alkoxysilane sols as hydrophobic treatments for concrete: A comparative study of bulk vs surface application," *Journal of Building Engineering,* vol. 46, p. 103729, 2022.

[8] X. Cao, F. Shu, S. Yan, B. Shi, K. Yao, and Q. Dong, "Design, preparation, and performance of a nano-modified organic-inorganic composite hydrophobic surface treatment agent for concrete," *Construction and Building Materials,* vol. 496, p. 143821, 2025.

[9] S. Jahandari, Z. Tao, M. A. Alim, and W. Li, "Integral waterproof concrete: A comprehensive review," *Journal of Building Engineering,* vol. 78, p. 107718, 2023.

[10] M. S. Hossain, V. Panov, S. Choi, J. B. kim, and K. K. Yun, "Durability performance of cement mortar incorporating water-repellent admixtures," *Construction and Building Materials,* vol. 440, p. 137262, 2024.

[11] K. Yahya, and H. Boussabaine, "Quantifying Environmental impacts and eco-costs from brick waste," *Architectural Engineering and Design Management,* vol. 6, no. 3, pp. 189–206, 2011.

[12] R. S. Mora-Ortiz, S. A. Diaz, E. Del Angel-Meraz, and F. Magana-hernandez, "Recycled fine aggregates from mortar debris and red clay brick to fabricate masonry mortars: mechanical analysis," *Materials (Basel),* vol. 15, no. 21, p. 7707, 2022.

[13] H. Wu, J. Xiao, C. Liang, and Z. Ma, "Properties of cementitious materials with recycled aggregate and powder both from clay brick waste," *Buildings,* vol. 11, no. 3, p. 119, 2021.

[14] Q. Liu, B. Li, J. Xiao, and A. Singh, "Utilization potential of aerated concrete block powder and clay brick powder from C&D waste," *Construction and Building Materials,* vol. 238, p. 117721, 2020.

[15] S. Beldjilali, A. Sarcinella, M. A. Ouared, A. Bougara, K. Naciri, and R.-M. Ion, "Waste brick as partial replacement of gypsum in mortars: Mechanical performance and environmental benefits for sustainable construction," *Sustainability,* vol. 17, no. 16, p. 7452, 2025.

[16] N. Kongkajun, E. A. Laitila, P. Ineure, W. Prakaypan, B. Cherdhirunkorn, and P. Chakartnarodom, "Soil-cement bricks produced from local clay brick waste and soft sludge from fiber cement production," *Case Studies in Construction Materials,* vol. 13, p. e00448, 2020.

[17] J. Shao, J. Gao, Y. Zhao, and X. Chen, "Study on the pozzolanic reaction of clay brick powder in blended cement pastes," *Construction and Building Materials,* vol. 213, pp. 209–215, 2019.

[18] X. Wang, W. Zhang, Y. Wang, H. Wu, D. Danzeng, and Y. Meng, "Assessment of the wettability and mechanical properties of stearic-acid-modified hydrophobic cementitious materials," *Coatings,* vol. 15, no. 1, p. 100, 2025.

[19] M. N. Chari, R. Naseroleslami, and M. Shekarchi, "The impact of calcium stearate on characteristics of concrete," *Asian Journal of Civil Engineering,* vol. 20, no. 7, pp. 1007–1020, 2019.

[20] F. Azarhomayun, M. Haji, M. Kioumarsi, and M. Shekarchi, "Effect of calcium stearate and aluminum powder on free and restrained drying shrinkage, crack characteristic and mechanical properties of concrete," *Cement and Concrete Composites,* vol. 125, p. 104276, 2022.

[21] M. S. Hossain, T. Ha, C. Song, and K. K. Yun, "Influence of water-repellent admixtures (Sitren and Stearate materials) on the microstructure and mechanical performance of conventional Portland cement paste and mortar," *Case Studies in Construction Materials,* vol. 21, p. e04036, 2024.

[22] L. Yang, Y. Pang, X. Chen, Q. Tang, H. Cui, D. Gao, ana M. Chen, "Effect of the stearic acid modified metakaolin on sulfate resistance of mortar based on the experimental study and capillary theory analysis," *Journal of Building Engineering,* vol. 71, p. 106513, 2023.

[23] Y. Pang, H. Wang, Q. Tang, L. Yang, and Q. Wang, "Enhancing cement mortar hydrophobicity against dry-wet cycling sulfate attack using stearic acid modified mica powder via high-temperature stirring," *Construction and Building Materials,* vol. 441, p. 137556, 2024.

[24] *ASTM C595 Standard Specification for Blended Hydraulic Cements*, 2021.

[25] *ASTM C136 Standard Test Method for Sieve Analysis of Fine and Coarse Aggregates*, 2025.

[26] *ASTM C642 Standard Test Method : Density, Absorptin and Voids for Hardened concrete*, 2022.

[27] *ASTM C109 Standard Test Method for Compressive Strength of Hydraulic Cement Mortars*. 2026.

[28] S. Sumiati, Mahmuda, Sukarman, S. Indra, and D. prabudi, "The utilization of crushed clay brick as coarse aggregate on eco-green lightweight foamed concrete," *Journal of Physics: Conference Series,* vol. 1500, no. 1, p. 012070, 2020.

[29] H. Katkhuda, and N. Shatarat, "Improving the mechanical properties of recycled concrete aggregate using chopped basalt fibers and acid treatment," *Construction and Building Materials,* vol. 140, pp. 328–335, 2017.

[30] C. Zhong, W. Lu, W. Mao, S. Xin, J. Chen, J, Zhou, and C. Shi, "Research on capillary water absorption characteristics of modified recycled concrete under different freeze–thaw environments," *Applied Sciences,* vol. 14, no. 3, p. 1247, 2024.

[31] R. Duarte, I. Flores-Colen, J. de Brito, and A. Hawreen, "Variability of in-situ testing in wall coating systems - Karsten tube and moisture meter techniques," *Journal of Building Engineering,* vol. 27, p. 100998, 2020.

[32] J. Wen, Y. Wan, and Y. Yang, "Sustainable synthesis of hydrophobic waste glass powder for enhanced water and frost resistance in mortar," *Construction and Building Materials,* vol. 487, p. 142097, 2025.

[33] S. Xu, Q. Wang, N. Wang, Q. Song, and Y. Li, "Effects of natural zeolite replacement on the properties of superhydrophobic mortar," *Construction and Building Materials,* vol. 348, p. 128567, 2022.

[34] S. M. Monteagudo, A. Moragues, J. C. Gálvez, M. J. Casati, and E. Reyes, "The degree of hydration assessment of blended cement pastes by differential thermal and thermogravimetric analysis: Morphological evolution of the solid phases," *Thermochimica Acta,* vol. 592, pp. 37–51, 2014.

[35] J. I. Bhatty, "Hydration versus strength in a portland cement developed from domestic mineral wastes — a comparative study," *Thermochimica Acta,* vol. 106, pp. 93–103, 1986.

[36] Z. Xu, W. Li, J, Sun, Y. Hu, K, Xu, S. Ma, and X. Shen, "Research

on cement hydration and hardening with different alkanolamines," *Construction and Building Materials,* vol. 141, pp. 296–306, 2017.

[37] N. Wang, Q. Wang, S. Xu, and L. Lei, "Green fabrication of mechanically stable superhydrophobic concrete with anti-corrosion property," *Journal of Cleaner Production*, vol. 312, p. 127836, 2021.